Climate Dynamics (1999) 15:341–354 

O. Marchal · T. F. Stocker · F. Joos · A. Indermühle
T. Blunier · J. Tschumi

# Modelling the concentration of atmospheric $CO_2$ during the Younger Dryas climate event

Received: 27 May 1998 / Accepted: 5 November 1998

**Abstract** The Younger Dryas (YD, dated between 12.7–11.6 ky BP in the GRIP ice core, Central Greenland) is a distinct cold period in the North Atlantic region during the last deglaciation. A popular, but controversial hypothesis to explain the cooling is a reduction of the Atlantic thermohaline circulation (THC) and associated northward heat flux as triggered by glacial meltwater. Recently, a $CH_4$-based synchronization of GRIP $\delta^{18}O$ and Byrd $CO_2$ records (West Antarctica) indicated that the concentration of atmospheric $CO_2$ ($CO_2^{atm}$) rose steadily during the YD, suggesting a minor influence of the THC on $CO_2^{atm}$ at that time. Here we show that the $CO_2^{atm}$ change in a zonally averaged, circulation-biogeochemistry ocean model when THC is collapsed by freshwater flux anomaly is consistent with the Byrd record. Cooling in the North Atlantic has a small effect on $CO_2^{atm}$ in this model, because it is spatially limited and compensated by far-field changes such as a warming in the Southern Ocean. The modelled Southern Ocean warming is in agreement with the anti-phase evolution of isotopic temperature records from GRIP (Northern Hemisphere) and from Byrd and Vostok (East Antarctica) during the YD. $\delta^{13}C$ depletion and $PO_4$ enrichment are predicted at depth in the North Atlantic, but not in the Southern Ocean. This could explain a part of the controversy about the intensity of the THC during the YD. Potential weaknesses in our interpretation of the Byrd $CO_2$ record in terms of THC changes are discussed.

O. Marchal (✉) · T. F. Stocker · F. Joos · A. Indermühle · T. Blunier · J. Tschumi
Climate and Environmental Physics, Physics Institute, University of Bern, Sidlerstrasse 5, 3012 Bern, Switzerland
E-mail: marchal@climate.unibe.ch

## 1 Introduction

Pollen continental sequences indicate that the Younger Dryas cold climate event of the last deglaciation (YD) affected mainly northern Europe and eastern Canada (Peteet 1995). This event has been dated by annual layer counting between $12\,700 \pm 100$ y BP and $11550 \pm 70$ y BP in the GRIP ice core (72.6 °N, 37.6 °W; Johnsen et al. 1992) and between $12\,940 \pm 260$ y BP and $11\,640 \pm 250$ y BP in the GISP2 ice core (72.6 °N, 38.5 °W; Alley et al. 1993), both drilled in Central Greenland. A popular hypothesis for the YD is a reduction in the formation of North Atlantic Deep Water by the input of low-density glacial meltwater, with a consequent weakening of the Atlantic thermohaline circulation (THC) and poleward heat transport (Broecker et al. 1985). This hypothesis is supported by cold sea surface temperatures in the North Atlantic at that time documented by the dominance of polar foraminiferal assemblages (Ruddiman and McIntyre 1981; Lehman and Keigwin 1992) and various model simulations which show that a weakening of the THC promotes a strong cooling in the North Atlantic region (Wright and Stocker 1993; Manabe and Stouffer 1995, 1997; Fanning and Weaver 1997; Mikolajewicz et al. 1997; Schiller et al. 1997). The meltwater hypothesis has been questioned, on the other hand, because nutrient proxy records from deep sea sediments give conflicting results with regard to the THC intensity during the YD (Boyle and Keigwin 1987; Keigwin et al. 1991; Keigwin and Lehman 1994; Jansen and Veum 1990; Veum et al. 1992; Charles and Fairbanks 1992; Sarnthein et al. 1994) and the YD seemingly occurred during a period of reduced melting (Fairbanks 1989; Bard et al. 1996; but see Edwards et al. 1993 for an opposite evidence). These two counter-arguments, however, might not be very critical for the meltwater hypothesis for several reasons. First, the apparent contradiction between nutrient proxy records during the YD could result from

a different time resolution and sampling frequency in the deep sea cores (Boyle 1995). Second, these records come from different depths and locations in the Atlantic and could thus have monitored the properties of different water masses in the past (Jansen and Veum 1990). Third, various factors can potentially affect deep sea nutrient proxy records, in addition to changes in the proportion of end members (Charles et al. 1993; Mackensen et al. 1993; McCorkle et al. 1995). Finally, the large pre-YD melting could have decreased surface salinities in the North Atlantic to the point where the THC becomes vulnerable to the glacial meltwater input documented during the cold event (Broecker 1990).

Analyses of air trapped in Greenland and Antarctic ice revealed large and abrupt changes in the atmospheric $CH_4$ content during the last deglaciation (Blunier et al. 1997). These changes must have the same origin because the residence time of $CH_4$ in the atmosphere is one order of magnitude larger than the interhemispheric exchange time. This permits a synchronization of ice cores from the Northern and Southern Hemispheres with a theoretical accuracy of about 50 y (Blunier et al. 1997). Blunier et al. (1997) used this approach to put three different polar ice records on a common time scale: the $\delta^{18}O$ record from GRIP, the $CO_2$ and $\delta^{18}O$ records from Byrd (80 °S, 120 °W) , and the $\delta D$ record from Vostok (78.5 °S, 106.8 °E). We use $CO_2$ data from Byrd to reconstruct the concentrations of atmospheric $CO_2(CO_2^{atm})$ for two reasons. First, the accumulation rate at Byrd is relatively high for Antarctica, which provides a good resolution of the $CO_2$ record (Neftel et al. 1988; Indermühle 1997). Second, the mean scatter of $CO_2$ measurements from neighbouring samples in Byrd glacial ice ($\sigma \sim 4$ parts per million by volume, (ppmv); 5 ppmv for the YD interval; Neftel et al. 1988; Indermühle 1997) is comparable to the analytical uncertainty ($\sim 3$ ppmv). This indicates that Byrd glacial ice (including that of the transition) is not greatly affected by chemical reactions (natural artefacts) which can potentially alter the $CO_2$ content of entrapped air (Anklin et al. 1997). Thus, the glacial $CO_2$ record from Byrd represents likely changes in the concentration of atmospheric $CO_2$. The main results of the north-south synchronization (Fig. 1a–d) are that the evolution of temperatures in Greenland and Antarctica was in antiphase, and the long-term glacial-Holocene increase of $CO_2^{atm}$ was not interrupted during the YD (Blunier et al. 1997). The latter result has been recently confirmed by additional $CO_2$ measurements in the Byrd ice core with higher analytical precision (Indermühle 1997; open circles in Fig. 1d).

In a previous study (Marchal et al. 1998b), we have applied a zonally averaged, coupled ocean-atmosphere model including ocean biogeochemical cycling to simulate the changes in atmospheric temperature and $CO_2^{atm}$ in response to a freshwater-induced collapse of the

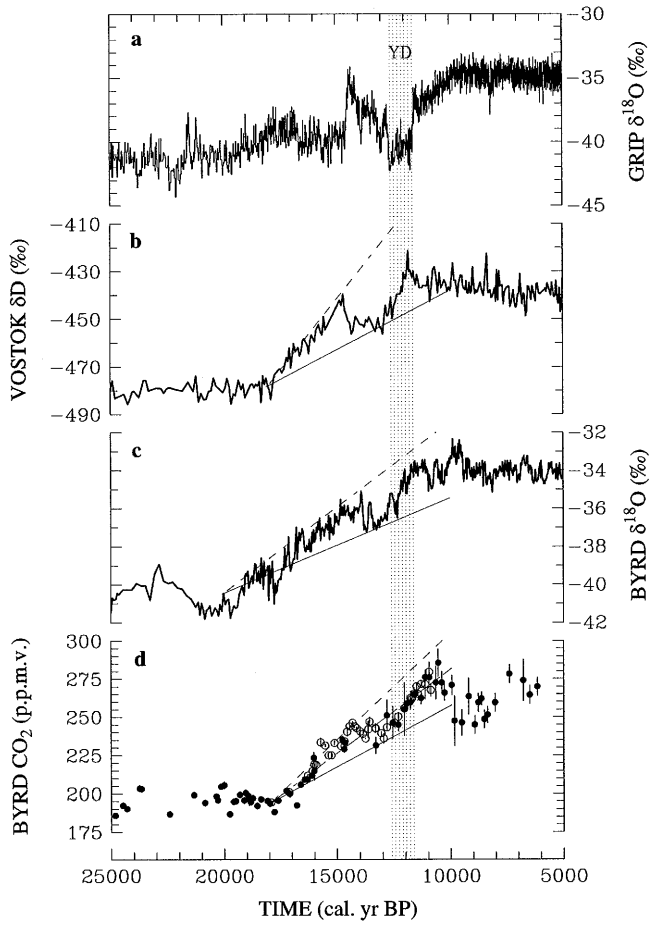


**Fig. 1a–d** Synchronized polar ice records during the last deglaciation: **a** $\delta^{18}O$ at GRIP (72.6°N, 37.6°W; data from Johnsen et al. 1992); **b** $\delta D$ at Vostok (78.5°S, 106.8°E; data from Jouzel et al. 1993); **c** $\delta^{18}O$ at Byrd station (80°S, 120°W; data from Johnsen et al. 1972); and **d** $CO_2$ at Byrd (mean $\pm 1\sigma$) (*solid circles*: data from Neftel et al. 1988; *open circles*: data from Indermühle 1997). The GRIP, Vostok and Byrd records are placed on a common chronology based on $CH_4$ changes measured in all records (Blunier et al. 1997, 1998) and using the GRIP time scale of Johnsen et al. (1992) as the reference. The *dashed area* indicates the Younger Dryas cold period (YD) in the GRIP record (12.7–11.6 ky BP). The *solid* and *dashed lines* in **b** correspond to long-term deglacial linear trends of respectively 5‰ $ky^{-1}$ and 12‰ $ky^{-1}$. The *solid* and *dashed lines* in **c** correspond to long-term deglacial linear trends of respectively 0.5‰ $ky^{-1}$ and 0.9‰ $ky^{-1}$. The *solid*, *long dashed*, and *short dashed lines* in **d** correspond to long-term deglacial linear trends of respectively 8 ppmv $ky^{-1}$, 11 ppmv $ky^{-1}$, and 14 ppmv $ky^{-1}$

THC. Here, we extend this study by a direct comparison of such changes with the isotopic records from GRIP, Byrd and Vostok, and with the $CO_2$ record from Byrd during the YD. Additional sensitivity experiments are also conducted.

The work is organized as follows. The model is briefly described in Sect. 2. We compare model results with polar ice core records in Sect. 3. Our interpretation of the Byrd $CO_2$ record in terms of THC changes is discussed in Sect. 4. and conclusions follow in Sect. 5.

## 2 Model description

A brief description of the model is given. Details can be found in Marchal et al. (1998 a,b). The model comprises physical and biogeochemical components. The physical component includes a zonally averaged global ocean circulation model (Wright and Stocker 1992): the Atlantic, Indian and Pacific basins are represented separately and connected in the south by a circumpolar channel (meridional and vertical widths of grid cells vary between 7.5°–15° and 50 m–500 m increasing with depth; for model grid see Stocker and Wright 1996). The ocean model is coupled to an energy balance model (EBM) of the atmosphere (Stocker et al. 1992) and a thermodynamic sea–ice model (Wright and Stocker 1993) in order to permit transitions between different climate states.

The biogeochemical component includes a description of organic matter and $CaCO_3$ cycling in the ocean and a 4-box land biosphere (Siegenthaler and Oeschger 1987). Nine oceanic tracers are considered (all in mol $m^{-3}$): phosphate (taken as the biolimiting nutrient), total dissolved inorganic carbon (DIC), alkalinity (ALK), labile dissolved organic carbon ($DOC_l$), dissolved oxygen, $^{13}C$ in DIC and $DOC_l$, and $^{14}C$ in DIC and $DOC_l$. Radiocarbon is included here as an organic tracer with fractionation factors for oceanic and land photosynthesis, and air–sea gas exchange equal to the square of the corresponding factors for $^{13}C$ (Craig 1954). The atmosphere is considered well mixed with regard to total $CO_2 (\equiv {}^{12}CO_2 + {}^{13}CO_2)$, $^{13}CO_2$, and $^{14}CO_2$. River input and sediment burial in the ocean are not taken into account, and $CO_2$ fluxes between the atmosphere and land biosphere and within the land biosphere are kept constant. Thus, in our experiments, anomalies in atmospheric $CO_2$ are only due to variations in the air–sea gas exchange, whereas anomalies in the atmospheric carbon isotope ratios are partly mitigated by $CO_2$ fluxes with the land biosphere. The model has been calibrated in order to reproduce the main features in the large-scale distribution of temperature, salinity, $\Delta^{14}C$ of DIC and major biogeochemical tracers in the modern oceans. It allows us to perform extensive sensitivity experiments with integration times of several thousand years.

We use a 6-step procedure in order to spin up the model to a steady state suitable for transient experiments (for details about the steady state, see Marchal et al. 1998a). First, sea surface temperatures (SST) and salinities are restored to modern annual zonal averages assuming that the Bølling warm interstadial which preceded the YD was a climate phase similar to the Holocene. We increase the restoring salinity value in the northernmost grid cell of the Atlantic and parameterize the effect of sea ice formation along the Antarctic perimeter in order to better represent the distributions of temperature, salinity and $\Delta^{14}C$ (of DIC) observed in the modern oceans. Climatological annual zonal averages of wind stress are applied in each basin. In the absence of reconstructions of surface nutrient concentration prior to the YD, the model $PO_4$ values in the ocean euphotic zone (top 100 m) are restored to annual zonal averages of $PO_4$ observed in the modern oceans, giving the production of organic carbon exported from the euphotic zone (export production). All other biological fluxes in the top 100 m and below are related stoichiometrically to the export production. We prescribe the chemical and isotopic conditions that prevailed before the YD as far as they are known. The atmospheric $CO_2$ is set to 240 ppmv (Neftel et al. 1988; Indermühle 1997), the atmospheric $\delta^{13}C$ to $-6.7‰$ (Leuenberger et al. 1992), and the atmospheric $\Delta^{14}C$ to 210‰ (Hughen et al. 1998). Second, we shift to mixed boundary conditions, i.e. the SSTs are still restored but water fluxes diagnosed at the surface are applied. This step allows us to verify that intermittent convection is not present during the spin-up. Third, the ocean mean salinity is increased by 1 as compared to modern conditions (Fairbanks 1990). Fourth, the model is coupled to the EBM and sea–ice model. Fifth, total $CO_2$, $^{13}CO_2$, and $^{14}CO_2$ are allowed to evolve freely in the atmosphere according to the exchange with the ocean surface and the land biosphere. Finally, in the last step, we adopt Michaelis-Menten kinetics to describe the export production as a function of $PO_4$ availability in the euphotic zone. All tracer fields are virtually unchanged after the first step.

In the model steady state, about 24 Sv of deep water ($1\ Sv = 10^6\ m^3\ s^{-1}$) are produced in the northern North Atlantic (Fig. 11a in Marchal et al. 1998b). About 8 Sv are exported to the Southern Ocean (south of 47.5°S), and then to the Indian and Pacific where broad upwelling occurs. The steady state also exhibits the transport of waters with low-DIC, high-$\delta^{13}C$ (low $PO_4$) and high-$\Delta^{14}C$ to depth in the northern North Atlantic, associated with NADW formation. These circulation, chemical and isotopic features are broadly consistent with observations in the modern oceans (Marchal et al. 1998a).

## 3 Results

We attempt to simulate a YD-like climate event by applying at the ocean surface a freshwater flux anomaly (FFA) equivalent to the first meltwater pulse of the last deglaciation (MWP-1A, at ~14 ky BP). This pulse is relatively well constrained in the Barbados coral record (Fairbanks 1990). Although MWP-1A preceded the onset of the YD by ~1 ky, it might have preconditioned the North Atlantic Ocean to YD cooling (Broecker 1990; Bard et al. 1996). The total volume and duration of the FFA are $7.2 \cdot 10^6 km^3$ and 500 y, based on a sea level rise of ~20 m between 14.2–13.7 ky BP identified from $^{230}Th/^{234}U$ ages of Barbados fossil corals (Table 1 in Fairbanks 1990). We assume a "triangular" shape of FFA from $t = 200$ y to 700 y in Figs. 2–5, i.e. a linear increase of 250 y and a subsequent linear decrease of 250 y. The exact location of meltwater discharge during MWP-1A is poorly known, as ice sheets from both the Northern Hemisphere and Antarctica could have contributed to it (Fairbanks et al. 1992; Clark et al. 1996). Here we describe experiments with different FFA allocations between 32.5°N–45°N in the Atlantic and 70°S–62.5°S along the Antarctic perimeter to check the sensitivity. We compare below model results with isotopic and $CO_2$ records from polar ice cores.

### 3.1 Comparison with isotopic records

#### *3.1.1 GRIP record*

The rate of thermohaline overturning in the Atlantic drops to 2 Sv and a strong cooling occurs at high northern latitude when at least 50% of the FFA are applied in the North Atlantic (dashed and thick solid lines in Fig. 2a). This is related to the build-up of a low-salinity cap in this region which reduces convection at high northern latitudes and poleward heat transport (Wright and Stocker 1993). The ~1 ky delay between MWP-1A and the onset of the YD (Bard et al. 1996) is not reproduced, which is a common shortcoming in model simulations of YD-like events (Wright and Stocker 1993; Manabe and Stouffer 1995; Mikolajewicz et al. 1997; Schiller et al. 1997). The duration of the period characterized by $\delta^{18}O$ minima in the GRIP ice

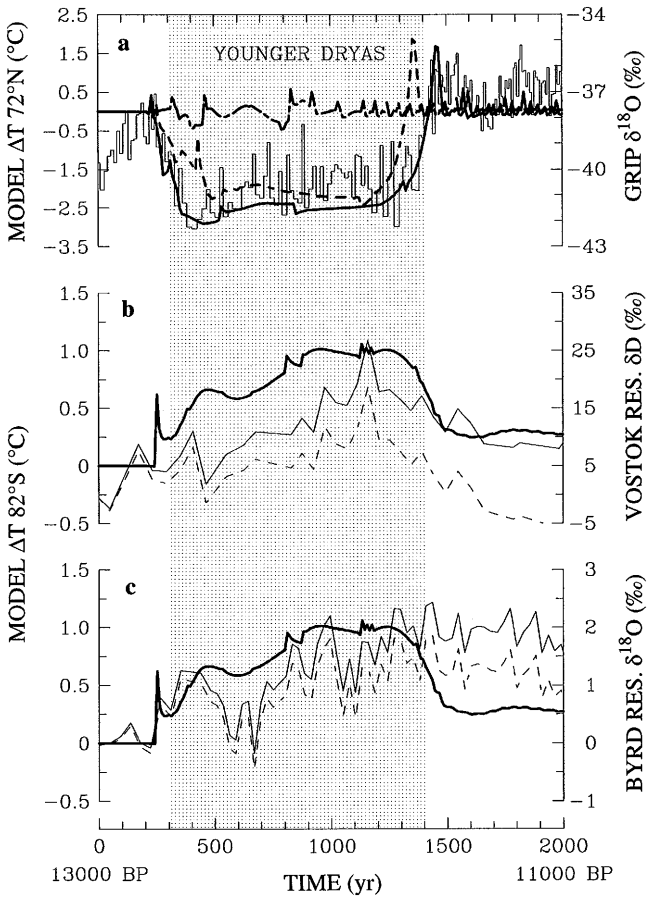


**Fig. 2a–c** Comparison of the model with ice core data. **a** $\delta^{18}O$ at GRIP (*thin solid line*; data from Johnsen et al. 1992); **b** residual $\delta D$ at Vostok relative to a glacial-Holocene $\delta D$ trend of 5‰ $ky^{-1}$ (*thin solid line*) and 12‰ $ky^{-1}$ (*dashed line*) (data from Jouzel et al. 1993); **c** residual $\delta^{18}O$ at Byrd station relative to a glacial-Holocene $\delta^{18}O$ trend of 0.5‰ $ky^{-1}$ (*thin solid line*) and 0.9‰ $ky^{-1}$ (*dashed line*) (data from Johnsen et al. 1972). The GRIP, Vostok and Byrd records are synchronized based on $CH_4$ changes measured in all records (Blunier et al. 1997) and taking the GRIP time scale of Johnsen et al. (1992) as the reference. They are plotted on an arbitrary time scale where $t = 0$ y and 2000 y correspond respectively to 13 000 y BP and 11 000 y BP in the GRIP record. The *dashed area* indicates the Younger Dryas cold period (YD) in the GRIP record (12.7–11.6 ky BP). In **a** the $\delta^{18}O$ record at GRIP is compared to the atmospheric temperature anomaly at 72.5 °N simulated when the freshwater flux anomaly (FFA) is applied entirely between 32.5 °N–45 °N in the Atlantic (*thick solid line*), equally between 32.5 °N–45 °N in the Atlantic and 70 °S–62.5 °S along the Antarctic perimeter (*dashed line*), and entirely between 70 °S–62.5 °S (*long-short dashed line*). In **b** and **c**, the residual $\delta D$ at Vostok and residual $\delta^{18}O$ at Byrd are compared to the atmospheric temperature anomaly at 82.5 °S simulated when the entire FFA is applied between 32.5 °N–45 °N in the Atlantic (*thick solid line*)

core (~1 ky) is best simulated when 100% of the FFA are applied in the North Atlantic (thick solid line in Fig. 2a). We will therefore concentrate on various aspects of this simulation. Note that the very good agreement between the observed and modeled duration of the cold event is probably fortuitous. Indeed this duration in the model depends strongly, for instance, on background water fluxes at the surface in the North Atlantic diagnosed during the spin-up (evaporation minus precipitation and runoff, kept constant in our experiments). When the entire FFA is applied along the Antarctic perimeter, a pronounced and persistent cold phase is not simulated at high northern latitudes (long-short dashed line in Fig. 2a).

We model a sudden resumption of the THC and a rapid warming at high northern latitudes. This is consistent with the very abrupt termination of the YD as documented in the GRIP $\delta^{18}O$ record (Fig. 2a; see also Dansgaard et al. 1989; Severinghaus et al. 1998). In the model, the background water fluxes at the surface and the ocean circulation gradually erode the low-salinity cap. The subsequent sudden resumption of the THC is due to the decrease of the stable salinity stratification in the northern North Atlantic to a point where it no longer counteracts the unstable temperature stratification. Warm and salty waters at depth are then mixed with the surface waters, which further destabilizes the water column and amplifies convection at high northern latitudes (Wright and Stocker 1991, 1993). The competition between the salinity and temperature stratifications could therefore be the threshold or trigger in the North Atlantic climate system hypothesized by Alley et al. (1993) to explain the extreme rapidity of the termination of the YD cold event.

### *3.1.2 Vostok and Byrd records*

In our model, the cooling at high northern latitudes, as triggered by the disruption of the northward heat flux, is accompanied by a warming at high southern latitudes (thick solid line in Fig. 2b–c). These results can be compared with the Vostok $\delta D$ record (Jouzel et al. 1993) and the Byrd $\delta^{18}O$ record (Johnsen et al. 1972) which were recently synchronized with the GRIP $\delta^{18}O$ record based on $CH_4$ measurements (Blunier et al. 1997). The model does not include all the processes necessary to simulate full glacial-interglacial climate transitions (continental ice sheets, for instance, are not represented). Thus, we compare model results with observed perturbations in the long-term trend of the glacial-Holocene transition. We subtract from Vostok $\delta D$ data ($\delta D_{Vostok}$) and Byrd $\delta^{18}O$ data ($\delta^{18}O_{Byrd}$) the long-term trend ($\overline{\Delta\delta D/\Delta t}$ and $\overline{\Delta\delta^{18}O/\Delta t}$) from the end of the last glacial period (18 ky BP for Vostok and 20 ky BP for Byrd) to the beginning of the Holocene (10 ky BP)

$$\delta D_{res} = \delta D_{Vostok} - \left(\overline{\frac{\Delta\delta D}{\Delta t}}\,[13ky - t_{i,\,Vostok}] - 454‰\right), \quad (1)$$

$$\delta^{18}O_{res} = \delta^{18}O_{Byrd} - \left(\overline{\frac{\Delta\delta^{18}O}{\Delta t}}\,[13ky - t_{i,\,Byrd}] - 36.65‰\right), \quad (2)$$

where $\delta D_{res}$ and $\delta^{18}O_{res}$ are the residual $\delta D$ and $\delta^{18}O$, $t_{i,\text{Vostok}}$ and $t_{i,\text{Byrd}}$ are the ages of the ice in the Vostok and Byrd cores, and $-454‰$ and $-36.65‰$ correspond approximately to the values of $\delta D$ and $\delta^{18}O$ at 13 ky BP in the Vostok and Byrd ice cores, respectively. Two different trends of $\overline{\delta D/\Delta t} = 5‰\,ky^{-1}$ and $12‰\,ky^{-1}$, $\overline{\Delta\delta^{18}O/\Delta t} = 0.5‰\,ky^{-1}$ and $0.9‰\,ky^{-1}$ are used to encompass the Vostok $\delta D$ and Byrd $\delta^{18}O$ records from 20–18 to 10 ky BP (Fig. 1b–c).

Both the Vostok $\delta D_{res}$ (East Antarctica) and Byrd $\delta^{18}O_{res}$ (West Antarctica) exhibit generally an increase during the YD (thin solid and dashed lines in Fig. 2b–c). The increase is 1 order of magnitude larger than the precision of $\delta D$ and $\delta^{18}O$ measurements (e.g. 0.3‰ for Vostok $\delta D$; Jouzel et al. 1987), indicating that it is due to changes in atmospheric conditions. This would suggest that a warming larger than the long-term warming of the last deglaciation occurred at Vostok and Byrd during the YD, provided that moisture sources, for instance, did not change markedly for this period.

The deuterium excess ($d = \delta D - 8{\cdot}\delta^{18}O$) has been related to the characteristics (relative humidity and sea surface temperature) of the moisture sources (Merlivat and Jouzel 1979; Johnsen et al. 1989) and could thus provide information on the variability of these sources at polar sites (Jouzel et al. 1982; Ciais et al. 1995). However, the time resolution of data available to calculate $d$ at Vostok and Byrd (Epstein et al. 1970; Lorius et al. 1985; Jouzel et al. 1987) is too coarse to identify a trend in the deuterium excess during the YD. The $d$ record at Dome C (74.6 °S, 124.2 °E) in East Antarctica has a higher resolution (Lorius et al. 1979; Jouzel et al. 1982). This record exhibits a significant rise of the deuterium excess from the end of the last ice age to the early Holocene (Jouzel et al. 1982). The Antarctic cold reversal was dated 1.3–1.7 ky younger in the Dome C $\delta D$ record (Jouzel et al. 1992) than in the Vostok and Byrd isotopic records (Blunier et al. 1997). We thus inspect $d$ changes occurring between 11.4–9.9 ky BP in the Dome C record in order to identify a possible significant trend during the YD. A two-tailed Mann test, based on the Kendall's tau coefficient (Kendall and Gibbons 1990), indicates no significant trend at the 1% probability level ($n = 24$; $P$-value $= 0.254$). Thus, the available $d$ records do not contradict the contention that the Vostok and the Byrd isotopic records during the YD reflect primarily temperature changes. Although the possibility of local effects cannot be excluded, the fact that the residual isotopic values increase at both stations would indicate a large-scale warming. The prediction of a warming at high southern latitudes during the cold phase in the Northern Hemisphere seems therefore consistent with Antarctic isotopic records during the YD. It is also consistent with SST reconstructions for this period from two sediment cores raised from the Indian sector of the Southern Ocean (Labracherie et al. 1989). In these reconstructions, however, the number of SST estimates during the YD (between 11–10 $^{14}$C-ky BP) is low (2–3 values) and cooling begins before the onset of the YD (11 $^{14}$C-ky BP). The cooling period subsequent to the warming in the model is indicated in the Vostok $\delta D$ record and Southern Ocean SST reconstructions (Labracherie et al. 1989), but not in the Byrd record (Fig. 2b–c).

### 3.2 Comparison with the Byrd $CO_2$ record

Important processes, such as ocean-sediment interaction which could have contributed to the long-term glacial-interglacial increases in $CO_2^{atm}$ during the late Pleistocene (Broecker and Peng 1991), are absent in our model. Thus, in order to compare the predicted $CO_2^{atm}$ with Byrd $CO_2$ data, we again subtract from these data the long term trend ($\overline{\Delta CO_2/\Delta t}$) from the end of the last glacial period (at 18 ky BP) to the beginning of the Holocene (10 ky BP) :

$$CO_2^{res} = CO_2^{Byrd} - \left(\overline{\frac{\Delta CO_2}{\Delta t}}\,[13\text{ ky} - t_{g,\text{Byrd}}] + 240\text{ ppmv}\right), \quad (3)$$

where $CO_2^{res}$ is the residual $CO_2$, $CO_2^{Byrd}$ are Byrd $CO_2$ data, $t_{g,\text{Byrd}}$ (in ky) is the age of the gas entrapped in the Byrd ice core, and 240 ppmv corresponds approximately to $CO_2^{atm}$ at 13 ky BP according to the Byrd $CO_2$ record. Different residual $CO_2$ quantities are calculated with various trends $\overline{\Delta CO_2/\Delta t}$ of 8, 11 and 14 ppmv·ky$^{-1}$ in order to encompass $CO_2$ values in the Byrd ice core from 18 to 10 ky BP (Fig. 1d)

The residual $CO_2$ values exhibit an increase during the YD with a peak-to-peak amplitude of 4–21 ppmv (filled and open circles in Fig. 3b–d). The range is due to the scatter of $CO_2$ measurements and to the uncertainty in $\overline{\Delta CO_2/\Delta t}$. Given this range, it is obvious that a quantitative interpretation of residual $CO_2$ during the YD documented in the Byrd ice core requires additional and precise $CO_2$ measurements from high-resolution ice cores. However, the Byrd $CO_2$ record does already provide evidence that the $CO_2^{atm}$ increase from the end of the last glacial period to the beginning of the Holocene has temporarily speeded up, or at least has not been interrupted during the YD.

We consider the mean difference between $CO_2^{res}$ and the simulated $CO_2^{atm}$ anomaly during the YD as a quantitative measure of the fit between the data and the model prediction. The difference ranges between 2–5 ppmv, depending on $\overline{\Delta CO_2/\Delta t}$, and indicates a reasonable fit to the ice core data (solid line in Fig. 3b–d). The major feature here is a simulated $CO_2^{atm}$ increase of 15 ppmv during the cold phase from $t = 500$ y to 1100 y (i.e. mostly after the FFA). The model does not reproduce the high-residual $CO_2$ at ~11.1 ky BP

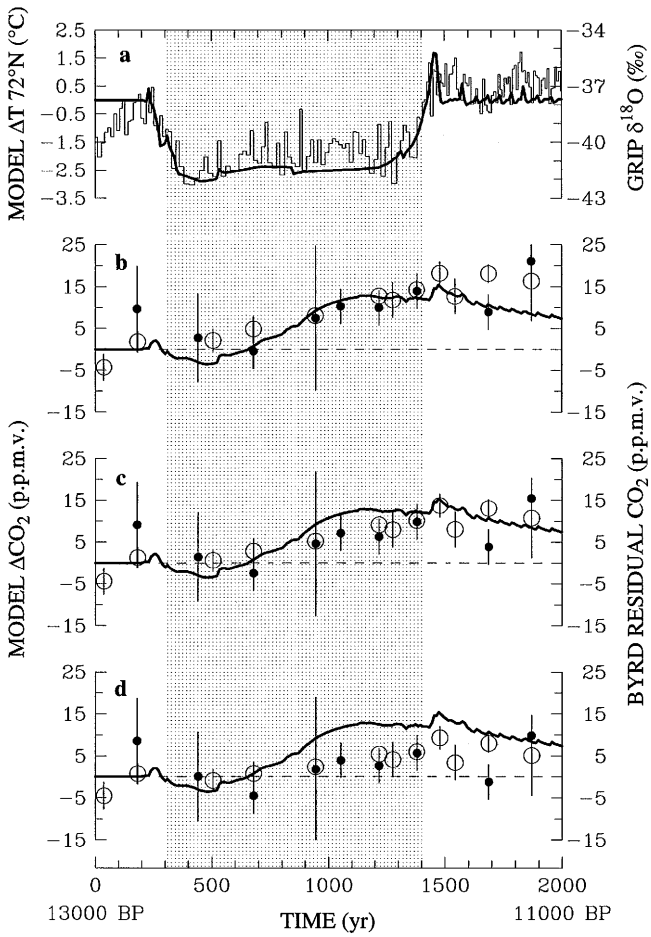


**Fig. 3a–d** Comparison of the model with ice core data. GRIP $\delta^{18}O$ record **a** (*thin solid line*; data from Johnsen et al. 1992); and residual $CO_2$ at Byrd station relative to a glacial-Holocene $CO_2$ trend of **b** 8 ppmv $ky^{-1}$, **c** 11 ppmv $ky^{-1}$ and **d** 14 ppmv $ky^{-1}$ (*filled circles*: data from Neftel et al. 1988; *open circles*: data from Indermühle 1997). $t = 0$ y and 2000 y correspond respectively to 13 000 y BP and 11 000 y BP in the GRIP record. The *dashed area* indicates the YD in this record. The $\delta^{18}O$ record at GRIP and the residual $CO_2$ record at Byrd are compared respectively to the atmospheric temperature anomaly at 72.5 °N and to the $CO_2^{atm}$ anomaly simulated when the entire FFA is applied between 32.5 °N–45 °N in the Atlantic (*thick solid line*)

calculated from the smallest glacial–Holocene trend of 8 ppmv $ky^{-1}$. The ice dated at ~11.1 ky BP in the Byrd core, however, exhibits a relatively large $CO_2$ scatter and a mean $CO_2$ content significantly higher than that measured on ice of the same age from Taylor Dome, a near-costal East Antarctic site (Indermühle et al. 1999). This suggests that the Byrd ice dated at ~11.1 ky BP might be affected by natural artefacts and would thus not reflect the atmospheric $CO_2$ content at that time. On the other hand, the model does not simulate the small residual $CO_2$ between 12.0–11.4 ky BP calculated from the longest trend of 14 ppmv $ky^{-1}$.

We identify the main factors responsible for the modeled $CO_2^{atm}$ increase. The simulated local partial pressure of $CO_2$ in the ocean mixed layer ($pCO_2$) is approximated as a linear combination of sea surface temperature (SST), salinity (SSS), DIC and ALK (Marchal et al. 1998b). The difference between the ocean mean linearized and simulated $pCO_2$ is ~1 µatm, i.e. an accuracy of 7% compared to the predicted $CO_2^{atm}$ increase. We estimate that about 50% of the $CO_2^{atm}$ increase (from $t = 500$ y to 1100 y) are due to a positive SSS anomaly, 30% to the net effect of the DIC and ALK changes, and 20% to warming. The positive SSS anomaly is due to the gradual erosion of the low-salinity cap at the surface in the Atlantic from the coldest model conditions at $t = 400$–500 y. The anomaly amounts to about +1 which results in a $CO_2^{atm}$ rise consistent with the thermodynamic effect calculated by Takahashi et al. (1993) (the global mean SSS rises by 0.6–0.7 in simulations where 50% and 100% of the FFA are applied along the Antarctic perimeter and offers similarly non negligible contributions to the $CO_2^{atm}$ increase which is also predicted in these simulations). On the other hand, the surface warming in the Southern Ocean (between 70 °S–47.5 °S, corresponding to 15% of total ocean area) reaches 1.6 °C, producing a local $pCO_2$ increase of ~16 µatm (Takahashi et al. 1993). It is sufficiently large to compensate the effect on $CO_2^{atm}$ of the 2.7 °C cooling north of 20 °N in the Atlantic (9% of total ocean area), which produces a local $pCO_2$ decrease of 27 µatm.

We have conducted sensitivity experiments in order to test whether the model simulates systematically a $CO_2^{atm}$ increase when the THC is disrupted (Table 1). Poorly-constrained parameters governing the air–sea gas exchange, the ocean biological cycling, and the potential DIC and ALK fluxes at the surface associated with the FFA are changed individually. We find a very small sensitivity (~1 ppmv) of the $CO_2^{atm}$ increase to the parametrization of the air–sea $CO_2$ exchange (constant or wind speed dependent transfer coefficient) and to a ±50% change in the restoring time for $PO_4$ in the euphotic zone (used during the model spin-up and determining the maximum rates of export production in the transient experiments), in the half-saturation constant for $PO_4$, and in the ocean mean $CaCO_3$: organic C production ratio. We must note, however, that wind speeds (and wind stresses) are kept constant in our experiments (there is no dynamics in the atmospheric model) and that zonal wind speeds over the Northern Hemisphere oceans might well have increased during the YD through an enhanced north–south pressure gradient as shown in different simulations of YD-like events (Fanning and Weaver 1997; Mikolajewicz et al. 1997; Schiller et al. 1997). The $CO_2^{atm}$ increase is also insensitive (±1 ppmv) to a change in the ocean mean content of labile dissolved organic carbon ($DOC_l$) between 5–20 mmol $m^{-3}$ and to a situation where the DIC and ALK of the

**Table 1** Summary of experiments

| | | | $\Delta CO_2^{atm\,a}$ | Byrd–model[b] |
|---|---|---|---|---|
| Reference experiment[c] | | | 15 | 2–5 |
| Air-sea $CO_2$ transfer coefficient ($\mu$) | variable[d] | mmol m$^{-2}$ y$^{-1}$ µatm$^{-1}$ | 16 | 2–6 |
| Restoring time for $PO_4$ in euphotic zone ($\tau_{PO_4}$) | 50 | d | 16 | 3–6 |
| | 150 | – | 15 | 2–4 |
| Half saturation constant for $PO_4$ uptake ($K_{PO_4}$) | 0.2 | mmol m$^{-3}$ | 15 | 2–4 |
| | 0.6 | – | 16 | 2–5 |
| Fraction of reduced C in $DOC_l$ ($\sigma$) [e] | 0.25 | 1 | 9 | 4–10 |
| | 0.75 | – | 24 | 7–12 |
| Ocean mean content of $DOC_l$ ($\overline{DOC_l}$) | 5 | mmol m$^{-3}$ | 14 | 2–5 |
| | 20 | – | 13 | 2–5 |
| Ocean mean $CaCO_3$ : organic C production ratio ($\overline{r_p}$) [f] | 0.03 | mol mol$^{-1}$ | 15 | 2–4 |
| | 0.09 | – | 16 | 3–6 |
| Dilution factor for the FFA ($\phi$) [g] | 0.4 | 1 | 15 | 2–5 |

[a]Peak-to-peak amplitude in atmospheric $CO_2$ concentration between $t = 300$ y and 1400 y (in ppmv)

[b]Mean difference between Byrd residual $CO_2$ and simulated atmospheric $CO_2$ concentration anomaly (in ppmv)

[c]$\mu = 67$ mmol m$^{-2}$ y$^{-1}$ µatm$^{-1}$, $\tau_{PO_4} = 100$ d, $K_{PO4} = 0.4$ mmol m$^{-3}$, $\sigma = 0.5$, $\overline{DOC_l} = 10$ mmol m$^{-3}$, $\overline{r_p} = 0.06$, and $\phi = 0$

[d]Calculated as a function of latitude in each basin from the zonally averaged climatological wind speeds of Esbensen and Kushnir (1981) using the formula of Tans et al. (1990)

[e]Biologically labile dissolved organic carbon

[f]Calculated from Eq. (14) in Marchal et al. (1998a) for a range in temperature from $-2$ to 30 °C

[g]Potential DIC and ALK fluxes at the surface associated with the FFA (m$^3$ s$^{-1}$) are included and calculated respectively as FFA·DIC(surf) /$\bar{S}\phi$ and FFA·ALK(surf) /$\bar{S}\phi$, where DIC(surf) and ALK(surf) are the local concentrations of DIC and ALK in the surface water, $\bar{S}$ is the ocean mean salinity, and $\phi$ (dimensionless) is a dilution factor. A value of 0.4 for $\phi$ means that the DIC and ALK of discharged water are 40% of the DIC and ALK of the ocean surface water. This value corresponds to the ratio between the concentration of $HCO_3^-$ in mean river water and mean ocean water today (Holland, 1978)

freshwater flux anomaly amount to 40% that of the ocean surface water (Table 1). By contrast, we observe a much larger sensitivity (~15 ppmv) to a change between 0.25–0.75 in the fraction of organic C sequestered into $DOC_l$. Even in this case, however, $CO_2^{atm}$ rises during the model cold phase (between 9–24 ppmv). Thus all these sensitivity experiments exhibit a positive $CO_2^{atm}$ anomaly, with a mean difference with Byrd residual $CO_2$ between 2–12 ppmv.

## 4 Discussion

We have shown that the anomalies of surface air temperature at 72.5 °N and 82.5 °S and the anomaly of atmospheric $CO_2$ concentration simulated in response to a drastic reduction of the THC compare favourably with ice core records during the Younger Dryas climate event. The GRIP, Vostok, and Byrd isotopic profiles document a thermal antiphasing between Greenland and Antarctica at that time, in line with the antiphasing observed in the same records during the Greenland warming events at ~45 and 36 ky BP (Blunier et al. 1998). Very recently, however, it was shown that the $\delta$D record from the near-costal site Taylor Dome exhibits a sudden rise and a period of minima which are synchronous with respectively the onset of the Bølling (at ~14.8 ky) and the YD in the GISP2 $\delta$D record [Steig et al. 1998]. Thus, rapid climate changes in Antarctica might not have been regionally uniform during the last deglaciation.

The continuous rise of $CO_2^{atm}$ during the YD, on the other hand, could have profound implications for the prediction of future $CO_2^{atm}$ levels. First, anthropogenic $CO_2$ has already penetrated deeply into the ocean interior in the North Atlantic (Gruber 1998). This suggests that NADW formation can be a major conduit of anthropogenic $CO_2$ from the atmosphere to the deep sea. Second, models of different complexity indicate that NADW formation may again be reduced during future centuries in response to the foreseen global warming (Manabe and Stouffer 1993; Stocker and Schmittner 1997). Clearly, the verification of the

present model scenario would be more convincing if a longer period was considered (e.g. 13–10 ky BP instead of 13–11 ky BP in this study). Two lines of evidence, however, suggest that the Byrd ice dated between about 11–10 ky BP might be altered by natural artefacts and would thus not represent past levels of atmospheric $CO_2$. First, replicate $CO_2$ measurements at depths corresponding to ages of 10 956 and 10 880 y BP exhibit a large scatter compared to older ice (Indermühle 1997). Second, $CO_2$ measurements in Byrd ice dated between 11–10 ky BP are significantly higher than $CO_2$ measurements on ice of the same age from Taylor Dome. The Taylor Dome $CO_2$ data are scarce ($n = 5$) and do not reveal a clear trend during that time interval (Indermühle et al. 1999). Thus, more $CO_2$ data from high-resolution polar ice cores are required in order to verify further our model results. We discuss potential weaknesses in our interpretation of the Byrd residual $CO_2$ in terms of ocean circulation changes in the next subsections.

### 4.1 Deep sea records of benthic foraminiferal $\delta^{13}C$ and Cd/Ca

Our model, as well as more complete coupled ocean-atmosphere three-dimensional circulation models which reproduce a YD-like event, exhibit a drastic reduction of the THC (Manabe and Stouffer 1995, 1997; Schiller et al. 1997; Mikolajewicz et al. 1997). This is supported by the $\delta^{13}C$ decrease and Cd/Ca increase in the bottom North Atlantic during the YD documented in several deep sea cores (Boyle and Keigwin 1987; Keigwin et al. 1991; Keigwin and Lehman 1994). Other $\delta^{13}C$ records from North Atlantic sediments, however, do not indicate such a reduction (Jansen and Veum 1990; Veum et al. 1992; Sarnthein et al. 1994). Conflicting $\delta^{13}C$ and Cd/Ca records from North Atlantic sediments might be due, among other things, to the fact that these records reflect changes in the properties of different water masses (Jansen and Veum 1990). Southern Ocean sediments should be less influenced by this effect, and it was argued that they could provide the most comprehensive measure of NADW flux variability where there is disagreement between nutrient proxy records from the Atlantic (Charles and Fairbanks 1992).

A strong $\delta^{13}C$ depletion during the YD is not found in Southern Ocean sediments (Charles et al. 1996), which would be interpreted as unaltered NADW flux at that time. This is illustrated by the benthic $\delta^{13}C$ record from core RC11-83 raised from the Atlantic sector of this basin (dots in Fig. 4a). Similarly, although THC is shut-down, our model does not predict $\delta^{13}C$ depletion and $PO_4$ enrichment in the deep Southern Ocean (thick line in Fig. 4a,b), consistent with this record. Such anomalies are simulated, on the other hand, in the deep North Atlantic (dashed line in Fig. 4a,b), which may

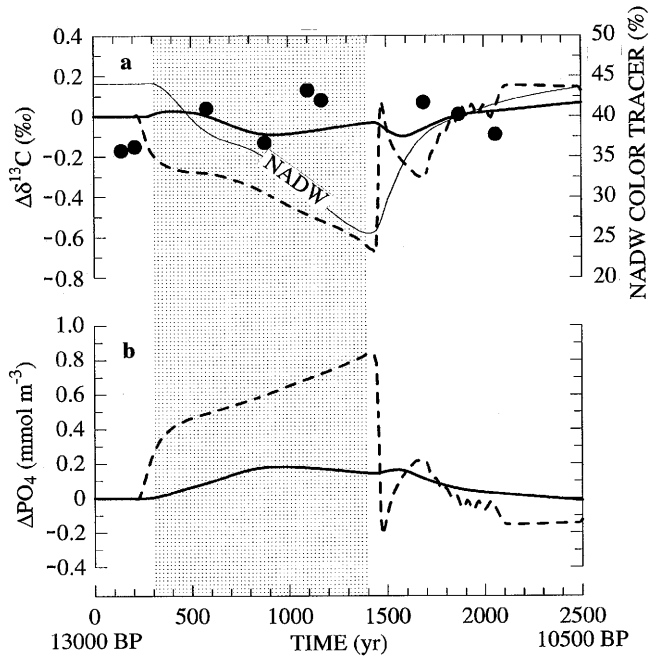


**Fig. 4a, b** Time series of **a** $\delta^{13}C$ and **b** $PO_4$ anomalies simulated at 3750 m in the Southern Ocean (51.25 °S; *thick solid lines*) and in the North Atlantic (50 °N; *dashed lines*). The entire FFA is applied between 32.5 °N–45 °N in the Atlantic. In **a** the dots correspond to the benthic foraminiferal $\delta^{13}C$ record of core RC11-83 in the Southern Ocean (41.4 °S, 94.5 °E; 4718 m; data from Charles and Fairbanks (1992) with measurement reproducibility $< 0.1‰$). The time scale in RC11-83 is constrained by calendar ages of 11.83 ky BP at a depth 189 cm and 13.01 ky BP at a depth of 221 cm (Charles et al. 1996) and assuming a constant sedimentation rate between these two dates. The anomalies of benthic foraminiferal $\delta^{13}C$ are calculated from a $\delta^{13}C$ value of 0.06‰ at ~13 ky BP corresponding to $t = 0$ y in the figure (Charles and Fairbanks 1992; Charles et al. 1996). The *thin solid line* is the modelled evolution of the NADW color tracer at 3750 m and 51.25 °S in the Southern Ocean (expressed as a percentage of its "concentration" at the location where this water mass is ventilated between 55 °N–80 °N). The *dashed area* indicates the YD in the GRIP record

safely be interpreted as reduced ventilation by NADW (Marchal et al. 1998b). The reduced influence of NADW in the Southern Ocean is illustrated by a drop of ~20% of the associated color tracer (thin solid line in Fig. 4a). The lack of a predicted $\delta^{13}C$ depletion and $PO_4$ enrichment in the Southern Ocean must therefore be related to the net effect of biological cycling (+ air–sea gas exchange for $\delta^{13}C$) which masks this reduced influence. The fact that the same THC change imparts very distinct $\delta^{13}C$ and $PO_4$ anomalies in the deep North Atlantic and Southern Ocean could have profound implications for the conventional interpretation of deep sea $\delta^{13}C$ and Cd/Ca records in locations distant from North Atlantic. These are beyond the scope of this study, but we do mention here that this might explain a part of the controversy about the intensity of the THC during the YD.

### 4.2 Records of atmospheric $\Delta^{14}C$

The atmospheric $\Delta^{14}C$ ($\Delta^{14}C_{atm}$) is mainly determined by $^{14}C$ production in the upper atmosphere (depending on cosmic ray flux, solar activity, and geomagnetic field intensity) and by $^{14}CO_2$ exchange with the ocean (rate of air–sea $^{14}CO_2$ flux and ocean ventilation). Analysis of fossil corals and varved sediments indicates that the $\Delta^{14}C_{atm}$ exhibited at first a rise, synchronous with the onset of the YD, and then a gradual decrease which ceased only after this cold event (Edwards et al. 1993; Goslar et al. 1995; Björck et al. 1996; Hughen et al. 1998; Kitagawa and van der Plicht 1998). In order to interpret the $\Delta^{14}C_{atm}$ record, Goslar et al. (1995) and Hughen et al. (1998) calculated the residual $\Delta^{14}C_{res} = \Delta^{14}C - \Delta^{14}C_{geo}$, where $\Delta^{14}C_{geo}$ is the $\Delta^{14}C_{atm}$ expected from past changes in the geomagnetic field strength. These authors showed that the long-term $\Delta^{14}C_{atm}$ decrease can be explained to a large extent by changes in $^{14}C$ production caused by variations in the Earth's dipole moment. However, they argued that the relatively fast changes of $\Delta^{14}C_{res}$ at the onset and during the YD cannot be explained by fluctuations in the geomagnetic field strength alone and were likely caused by ocean ventilation changes.

We compare the $\Delta^{14}C_{atm}$ anomaly simulated by our model (where $^{14}C$ production is constant; Stocker and Wright 1996) with the residual $\Delta^{14}C_{res}$ based on the recent $\Delta^{14}C$ record from the varved sediment core of the Cariaco Basin (Hughen et al. 1998). Two different time series of $\Delta^{14}C_{res}$ are considered in an attempt to account for the large uncertainties in the reconstruction of geomagnetic field intensities (Tric et al. 1992; Guyoda and Valet 1996; Laj et al. 1996; Frank et al. 1997). A first time series is obtained assuming a linear decrease of $\Delta^{14}C_{geo}$ of 50‰ from 13 ky BP to 11 ky BP (open circles in Fig. 5). This scenario is an approximation of the $\Delta^{14}C_{geo}$ calculated by Goslar et al. (1995), and used later by Hughen et al. (1998), on the basis of the reconstruction of the Earth's dipole moment by Tric et al. (1992). A second time series of $\Delta^{14}C_{res}$ is obtained by assuming that the production of atmospheric $^{14}C$ has not changed between 13–11 ky BP, i.e. $\Delta^{14}C_{geo}$ is constant (solid circles in Fig. 5). This is supported by the absence of a significant trend in the geomagnetic field strength during this period according to a recent and high-resolution synthetic record (Laj et al. 1996). The Cariaco Basin varve chronology, on the other hand, is slightly modified in order to ensure comparability with the YD as dated in the GRIP time scale (taken here as the reference). The onset and termination of the YD in the varve chronology were dated at ~13000 y BP and 11 700 y BP, respectively (Hughen et al. 1998). These dates are similar to those of the YD in the GISP2 ice core (Alley et al. 1993), but older by respectively ~300 y and 100 y than those of the YD in the GRIP ice core (Johnsen et al. 1992). Thus, we subtract from the Cariaco Basin chronology a value ranging from 300 y for varve age 13000 y BP to 100 y for varve age 11 700 y BP (linear squeezing). Outside the period 13 000–11 700 y BP in the original varve chronology, a constant value is subtracted from the varve ages depending on the original age differences. Taking the varve chronology as the reference time scale does not alter our main conclusion below.

As in previous simulations with our zonally averaged model (Stocker and Wright 1996) and 3-D ocean circulation model (Mikolajewicz 1996), the simulated

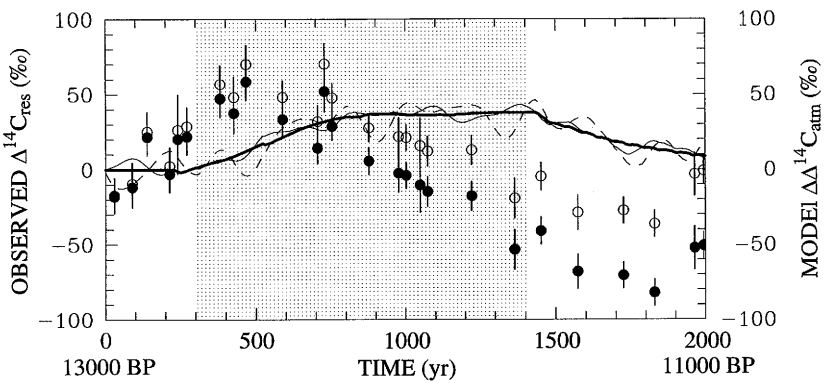


**Fig. 5** Atmospheric residual $\Delta^{14}C_{res}$ according to the varved sediment record from the Cariaco Basin (10.7 °N, 65 °W; $\Delta^{14}C$ data from Hughen et al. 1998). A first time series of $\Delta^{14}C_{res}$ (*open circles*) is calculated assuming a linear decrease of $\Delta^{14}C_{geo}$ from 210‰ at 13 ky BP ($t = 0$ y in the figure) to 160‰ at 11 ky BP ($t = 2000$ y). A second time series (*solid circles*) is calculated assuming a constant $\Delta^{14}C_{geo}$ of 210‰. *Vertical bars* denote uncertainties of $\Delta^{14}C$ measurements ($\pm 1\sigma$). The varved ages of Hughen et al. (1998) are modified in order to compare consistently the $\Delta^{14}C_{geo}$ record with the YD in the GRIP record (corresponding to the *dashed area*). The *three lines* are atmospheric $\Delta^{14}C$ anomalies simulated by the model with the entire FFA applied between 32.5 °N–45 °N in the Atlantic. The *thick line* corresponds to the case where $^{14}C$ production is kept constant. The *thin dashed* and *solid lines* correspond to cases where $^{14}C$ production changes according to Eqs. (1) and (2) of Stuiver and Braziunas (1989), respectively. These equations approximate different sections of the Holocene record of solar-induced changes in atmospheric $^{14}C$ production: the first equation is valid for four episodes of triple oscillations containing at least two of the Maunder- and Spörer $\Delta^{14}C_{atm}$ maxima (covering ~30% of the entire Holocene $\Delta^{14}C_{atm}$ record) and the second is valid for the remaining sections of the record

$\Delta^{14}C_{atm}$ increases when the THC weakens (thick solid line in Fig. 5). This is consistent with the $\Delta^{14}C_{res}$ rise synchronous with the initiation of the YD documented in the Cariaco Basin record, even if the original varve chronology is considered given dating uncertainties (Hughen et al. 1998). The predicted increase of $\sim 40‰$ is smaller than that in the Cariaco Basin record, but it must be noted that the Cariaco Basin $\Delta^{14}C$ in the initial phase of the YD are significantly higher than in other $\Delta^{14}C$ records (Fig. 4 in Hughen et al. 1998). On the other hand, our model, as well as other simulations (Stocker and Wright 1996; Mikolajewicz 1996), does not reproduce the subsequent $\Delta^{14}C_{res}$ decrease during the second half of the cold phase (Fig. 5). Box models showed that such a decrease can be produced by an increase in the gas exchange rate and/or gradual recovery of the THC during the cold phase (Björck et al. 1996; Hughen et al. 1998). The first effect is consistent with increasing wind speeds over the Northern Hemisphere oceans predicted in different simulations of YD-like events (Fanning and Weaver 1997; Mikolajewicz et al. 1997; Schiller et al. 1997). Hughen et al. (1998), on the other hand, argued that an enhanced formation of Glacial North Atlantic Intermediate Water (GNAIW) during the YD could lead to the observed $\Delta^{14}C_{atm}$ decrease. A resuming GNAIW formation at that time is consistent with the benthic foraminiferal record of core OC205-2-103GGC (26.1 °N, 78 °W; 965 m) in the western North Atlantic documenting declining Cd/Ca values and hence efficient GNAIW ventilation during the YD (Marchitto et al. 1998). Broecker (1998), however, mentioned several deficiencies in the scenario of Hughen et al. (1998) and argued that increasing ventilation in the Southern Ocean was rather responsible for the $\Delta^{14}C_{atm}$ decrease. Another possible cause for this decrease would be enhanced $^{14}C$ uptake by North Pacific Intermediate Water during the YD, consistent with marine sediment records and a 3-D model simulation (see Mikolajewicz et al. 1997 and references therein).

The possibility that the $\Delta^{14}C_{res}$ records in Fig. 5 do not only reflect ocean ventilation changes cannot, on the other hand, be definitively excluded. For instance, subtracting a constant reservoir age from the Cariaco Basin record (420 y; Hughen et al. 1998) to correct for air–sea $^{14}C$ activity difference would not be appropriate if this difference changed significantly during the YD. Bard et al. (1994) measured $\Delta^{14}C$ on fossil terrestrial plants and marine planktonic foraminifera mixed with the same volcanic tephra and estimated that the $^{14}C$ age difference between the atmosphere and North Atlantic surface waters at 10 300 $^{14}C$ y BP was $\sim$700–800 y (instead of a pre-industrial value of 400–500 y). Using a reservoir age of 750 y instead of 420 y increases the Cariaco Basin $\Delta^{14}C_{res}$ by 47–58‰ between 13–11 ky BP (assuming that the basin geometry maintained a reservoir age near open-ocean values as today; Hughen et al. 1998). This worsens the model misfit in the early stage of the YD but improves it afterwards. There is no paleoclimate data, however, to test whether the assumption of a constant reservoir age during the YD is realistic (note that our model exhibits during the cold phase a peak-to-peak amplitude of $\sim$100 y in the reservoir age at the latitude of the Cariaco Basin). The resolution of geomagnetic paleointensity records, on the other hand, is typically not better than $\sim$1 ky (Guyodo and Valet 1996; Frank et al. 1997) so that possible fast $\Delta^{14}C_{geo}$ changes during the YD event cannot be detected. Solar oscillations appear as the main contributor to the century scale variability of $\Delta^{14}C_{atm}$ during the Holocene (Stuiver et al. 1991) but are not known for the last deglaciation. Stuiver and Braziunas (1989) derived a record of solar-induced changes of $^{14}C$ production based on $\Delta^{14}C$ measurements in Holocene trees dated by dendrochronology and a box model. We used this record in order to identify how these changes would have affected $\Delta^{14}C_{atm}$ during the YD. We conducted two experiments including an approximation of these changes for different sections of the Holocene record (thin dashed and solid lines in Fig. 5). The solar induced changes in $\Delta^{14}C_{atm}$ are too small and occur on a too short time scale to improve the fit between $\Delta^{14}C_{res}$ and the predicted $\Delta^{14}C_{atm}$ anomaly. Thus, if solar activity changes during the YD had a similar pattern to that of the Holocene, they would have had a negligible impact on the $\Delta^{14}C_{res}$ decrease which initiated at that time (Hughen et al. 1998). Although the amplitude of the model misfit to $\Delta^{14}C_{res}$ is difficult to assess given the uncertainties in atmospheric $^{14}C$ level and production rate during the YD, the present interpretation of Byrd residual $CO_2$ may need revision if this decrease really documents an enhanced $^{14}CO_2$ exchange with the ocean.

### 4.3 Rapidity of the circulation response and initial conditions

Other problems inherent to all simulations of YD-like events (Wright and Stocker 1993; Manabe and Stouffer 1995, 1997; Fanning and Weaver 1997; Mikolajewicz et al. 1997; Schiller et al. 1997) are the quasi-instantaneous response of the THC to freshwater flux anomaly and the choice of adequate initial conditions. In simulations where the FFA leading to THC disruption is equivalent to meltwater pulse MWP-1A (as here), the rapidity of the circulation response is inconsistent with the $\sim$1 ky delay between this pulse and the onset of the YD observed in the paleoclimate record (Bard et al. 1996). As pointed out by Broecker (1990), MWP-1A could have preconditioned the North Atlantic region to YD cooling by decreasing the sea surface salinities in this region. This would have made the THC much more sensitive to the reduced glacial meltwater fluxes which occurred after MWP-1A. Thus, provided that

the evolution of a low-salinity cap in the North Atlantic was the factor which ultimately triggered the onset and termination of the YD (Broecker 1990), the present interpretation of Byrd residual $CO_2$ should be viable. It is consistent with high-resolution records of planktonic $\delta^{18}O$ from North Atlantic sediments which document low SSS during the YD and high SSS afterwards (Duplessy et al. 1992).

Initial conditions in simulations of YD-like events correspond to the modern ones, which may be justified by the mild period (Bølling-Allerød interstadial complex) which preceded the YD (Mangerud et al. 1974; Johnsen et al. 1992). $\delta^{18}O$ records from Greenland ice cores (Johnsen et al. 1992) suggest that at the beginning of the Bølling ($\sim$14.4 ky BP in GRIP record) the temperature in the North Atlantic atmosphere and thus NADW production were similar to those of today. However, the same records document a gradual climate deterioration from this period which culminated with the onset of the YD ($\sim$12.7 ky BP in GRIP record). Thus, neither Greenland $\delta^{18}O$ records, nor pollen sequences from the North Atlantic region, do support *sensu stricto* the adoption of "modern" initial conditions in simulations of YD-like events. This remains a useful working hypothesis, however, given the poor observational constraints on climate conditions that prevailed just before the YD.

### 4.4 Other possible contributors to $CO_2^{atm}$ changes during the Younger Dryas

Effects other than changes in the deep ocean circulation could have contributed to the (relatively small) positive residual $CO_2$ during the YD. Coral records from Barbados, New Guinea, and Tahiti all document a rising sea level between 12.7–11.6 ky BP (see Fig. 2 in Bard et al. 1996). It is conceivable that possible sudden floodings of continental shelves at that time altered the atmospheric $CO_2$ content. A first effect would be through the sequestration of $PO_4$ in shelf sediments, thereby decreasing the ocean biological uptake of $CO_2$ and increasing $CO_2^{atm}$ (Broecker 1982). A second effect would be through an enhanced $CaCO_3$ deposition on tropical reefs and banks (Opdyke and Walker 1992; Kleypas 1997), which results in a lower alkalinity and a higher partial pressure of $CO_2$ (Frankignoulle et al. 1994). Finally, the inundation of lowland areas would have had consequences on carbon storage on land and hence on the net biospheric flux of $CO_2$ to the atmosphere (Esser and Lautenschlager 1994). Were the net effect of abrupt marine transgressions be dominant, we should observe a significant $CO_2^{atm}$ anomaly during the first meltwater MWP-1A (at $\sim$14 ky BP), which alone accounted for $\sim 1/6$ of the total sea level rise during the last deglaciation. The Byrd ice core documents a small $CO_2$ increase approximately at that time (Fig. 1d), but the number of data even in this high-resolution record is small. Changes in the net $CO_2$ uptake by terrestrial ecosystems that are not directly tied to the sea level rise could conceivably have also affected the concentration of atmospheric $CO_2$ during the YD. This hypothesis could be constrained e.g. through high-resolution pollen profiles or atmospheric $\delta^{13}C$ records which are not available at the present time.

## 5 Conclusions

The high-resolution $CO_2$ record from the Byrd ice core documents that the glacial-Holocene increase in the atmospheric $CO_2$ concentration has temporarily speeded up, or remained constant during the Younger Dryas cold climate event. The present observational evidence seems sufficiently strong to deserve investigation. It may have profound implications for the prediction of future $CO_2^{atm}$ levels for it suggests a minor influence of the North Atlantic on $CO_2^{atm}$. Here we have shown that the $CO_2^{atm}$ change predicted in a zonally averaged, circulation-biogeochemistry ocean model when perturbed by a freshwater flux anomaly is not inconsistent with the Byrd record. In this model, the surface cooling triggered by a collapse of the THC is not dominant on $CO_2^{atm}$, because it is confined to the North Atlantic and compensated by other responses such as a warming in the Southern Ocean. This latter response is consistent with Antarctic isotopic records during the YD. Potential weaknesses in our interpretation of Byrd residual $CO_2$ are the absence of a $\Delta^{14}C_{atm}$ drop during the cold phase at high northern latitudes, uncertainties of initial conditions, and the lack of a time lag between freshwater forcing and climatic response in the model. On the other hand, a strong nutrient enrichment is simulated at depth in the North Atlantic, but not in the Southern Ocean. This could at least partly resolve the controversy about the intensity of the THC during the YD. The present model scenario could be further verified by a precise determination from high-resolution archives of atmospheric $CO_2$ concentration, temperature changes in the Southern Ocean, and atmospheric $^{14}C$ activity and production rate during the Younger Dryas cold climate event.

**Acknowledgements** We are very grateful to K. Hughen for providing the Cariaco Basin $\Delta^{14}C$ record and for helpful discussions on the interpretation of this record. We are also indebted to B. Stauffer and one anonymous reviewer for useful comments on the manuscript. J. Jouzel provided Dome C records and information on the deuterium excess in Antarctic ice cores. We enjoyed a discussion with A. Mazaud on the reconstruction of geomagnetic intensities. This study was made possible by the Swiss National Science Foundation and grant BBW 95.0471 from European Projects ENV4-CT95-0131 "Variability of the Glacial and Interglacial Climates and Abrupt Climatic Changes" and ENV4-CT95-0130 "North-South Climatic Connection and Carbon Cycle over the last 250 ky".

## References


Alley RB, Meese DA, Shuman CA, Gow AJ, Taylor KC, Grootes PM, White JWC, Ram M, Waddington ED, Mayewski PA, Zielinski GA (1993) Abrupt increase in Greenland snow accumulation at the end of the Younger Dryas event. Nature 362 : 527–529

Anklin M, Schwander J, Stauffer B, Tschumi J, Fuchs A, Barnola J-M, Raynaud D (1997) $CO_2$ record between 40 and 8 ky BP from the Greenland ice core project ice core. J Geophys Res 102 : 26 539–26 545

Bard E, Arnold M, Mangerud J, Paterne M, Labeyrie L, Duprat J, Mélières M-A, Sønstegaard E, Duplessy J-C (1994) The North Atlantic atmosphere-sea surface $^{14}C$ gradient during the Younger Dryas climatic event. Earth Planet Sci Lett 126 : 275–287

Bard E, Hamelin B, Arnold M, Montaggioni L, Cabioch G, Faure G, Rougerie F (1996) Deglacial sea-level record from Tahiti corals and the timing of global meltwater discharge. Nature 382 : 241–244

Björck S, Kromer B, Johnsen S, Bennike O, Hammarlund D, Lemdahl G, Possnert G, Rasmussen B, Wohlfahrt B, Hammer CU, Spurk M (1996) Synchronised terrestrial-atmospheric deglacial records around the North Atlantic. Science 274 : 1155–1160

Blunier T, Chappellaz J, Schwander J, Dällenbach A, Stauffer B, Stocker TF, Raynaud D, Jouzel J, Clausen HB, Hammer CU, Johnsen SJ (1998) Asynchrony of Antarctic and Greenland climate change during the last glacial period. Nature 394 : 739–743

Blunier T, Schwander J, Stauffer B, Stocker T, Dällenbach A, Indermühle A, Tschumi J, Chappellaz J, Raynaud D, Barnola J-M (1997) Timing of temperature variations during the last deglaciation in Antarctica and the atmospheric $CO_2$ increase with respect to the Younger Dryas event. Geophys Res Lett 24 : 2683–2686

Boyle EA (1995) Last-Glacial-Maximum North Atlantic Deep Water: on, off or somewhere in-between? Philos Trans R Soc London 348 : 243–253

Boyle EA, Keigwin LD (1987) North Atlantic thermohaline circulation during the past 20,000 years linked to high-latitude surface temperature. Nature 330 : 35–40

Broecker WS (1982) Glacial to interglacial changes in ocean chemistry. Prog Oceanogr 11 : 151–197

Broecker WS (1990) Salinity history of the northern Atlantic during the last deglaciation. Paleoceanography 5 : 459–467

Broecker WS (1998) Paleocean circulation during the last deglaciation: a bipolar seesaw. Paleoceanography 13 : 119–121

Broecker WS, Peng T-H (1991) What caused the glacial to interglacial $CO_2$ change? In: Heimann M (ed) The global carbon cycle. Vol I 15 of NATO ASI Series, Springer-Verlag, Berlin, Heidelberg, New York, pp 95–115

Broecker WS, Peteet D, Rind D (1985) Does the ocean-atmosphere system have more than one stable mode of operation? Nature 315 : 21–25

Charles C, Fairbanks RG (1992) Evidence from Southern Ocean sediments for the effect of North Atlantic deep-water flux on climate. Nature 355 : 416–419

Charles CD, Lynch-Stieglitz J, Ninnemann US, Fairbanks RG (1996) Climate connections between the hemisphere revealed by deep sea sediment core/ice core correlations. Earth Planet Sci Lett 142 : 19–27

Charles CD, Wright JD, Fairbanks RG (1993) Thermodynamic influences on the marine carbon isotope record. Paleoceanography 8 : 691–697.

Ciais P, White JWC, Jouzel J, Petit J-R (1995) The origin of present-day Antarctic precipitation from surface snow deuterium excess data. J Geophys Res 100 : 18 917–18 927

Clark PU, Alley RB, Keigwin LD, Licciardi JM, Johnsen SJ, Wang H (1996) Origin of the first global meltwater pulse. Paleoceanography 11 : 563–577

Craig H (1954) Carbon 13 in plants and the relationship between carbon 13 and carbon 14 variations in nature. J Geol 62 : 115–149

Dansgaard W, White JWC, Johnsen SJ (1989) The abrupt termination of the Younger Dryas climate event. Nature 339 : 532–534

Duplessy J-C, Labeyrie L, Arnold M, Paterne M, Duprat J, Van Weering TCE (1992) Changes in surface salinity of the North Atlantic Ocean during the last deglaciation. Nature 358 : 485–488

Edwards RL, Beck WJ, Burr GS, Donahue DJ, Chappell JMA, Bloom AL, Druffel ERM, Taylor FW (1993) A large drop in atmospheric $^{14}C/^{12}C$ and reduced melting in the Younger Dryas, documented with $^{230}Th$ ages of corals. Science 260 : 962–968

Epstein S, Sharp RP, Gow AJ (1970) Antarctic ice sheet: Stable isotope analysis of Byrd station cores and interhemispheric climatic implications. Science 168 : 1570–1572

Esbensen SK, Kushnir Y (1981) The heat budget of the global ocean: an atlas based on estimates from marine surface observations. Rep 29, Climate Research Institution, Oregon State University, Oregon, USA

Esser G, Lautenschlager M (1994) Estimating the change of carbon terrestrial biosphere from 18 000 BP to present using a carbon cycle model. Environ Pollut 83 : 45–53

Fairbanks RG (1989) A 17 000 year glacio-eustatic sea-level record: influence of glacial melting rates on the Younger Dryas event and deep ocean circulation. Nature 342 : 637–642

Fairbanks RG (1990) The age and origin of the "Younger Dryas climate event" in Greenland ice cores. Paleoceanography 5 : 937–948

Fairbanks RG, Charles CD, Wright JD (1992) Origin of global meltwater pulses. In: Taylor EE et al. (eds) Radiocarbon after four decades. Springer-Verlag, New York, Berlin, Heidelberg, pp 473–500

Fanning AF, Weaver AJ (1997) Temporal-geographical meltwater influences on the North Atlantic conveyor: implications for the Younger Dryas. Paleoceanography 12 : 307–320

Frank M, Schwarz B, Baumann S, Kubik PW, Suter M, Mangini A (1997) A 200 ky record of cosmogenic radionuclide production rate and geomagnetic field intensity from $^{10}Be$ in globally stacked deep-sea sediments. Earth Planet Sci Lett 149 : 121–129

Frankignoulle M, Canon C, Gattuso J-P (1994) Marine calcification as a source of carbon dioxide: positive feedback of increasing atmospheric $CO_2$. Limnol Oceanogr 39 : 458–462

Goslar T, Arnold M, Bard E, Kuc T, Pazdur MF, Ralska-Jasiewiczowa M, Różański K, Tisnerat N, Walanus A, Wicik B, Więckowski K (1995) High concentration of atmospheric $^{14}C$ during the Younger Dryas cold episode. Nature 377 : 414–417

Gruber N (1998) Anthropogenic $CO_2$ in the Atlantic Ocean. Global Biogeochem Cycles 12 : 165–196

Guyodo Y, Valet J-P (1996) Relative variations in geomagnetic intensity from sedimentary records: the past 200 000 years. Earth Planet Sci Lett 143 : 23–36

Holland HD (1978) The chemistry of the atmosphere and oceans. Wiley-Interscience, New York

Hughen KA, Overpeck JT, Lehman SJ, Kashgarian M, Southon J, Peterson LC, Alley R, Sigman DM (1998) Deglacial changes in ocean circulation from an extended radiocarbon calibration. Nature 391 : 65–68

Indermühle A (1997) $CO_2$ Konzentrationsmessungen an polaren Eisproben insbesondere am Eisbohrkern von Byrd Station, Antarktis, Diplomarbeit, Physikalisches Institut der Universität Bern, Universität Bern, Bern, Switzerland

Indermühle A, Stocker TF, Joos F, Fisher H, Smith HJ, Wahlen M, Deck B, Mastroianni D, Tschumi J, Blunier T, Meyer R, Stauffer B (1999) Holocene carbon cycle based on a high-resolution $CO_2$ ice core record from Taylor Dome, Antarctica. Nature (in press)

Jansen E, Veum T (1990) Evidence for two-step deglaciation and its impact on North Atlantic deep-water circulation. Nature 343 : 612–616

Johnsen SJ, Dansgaard W, Clausen HB, Langway CC (1972) Oxygen isotope profiles through the Antarctic and Greenland ice sheets. Nature 235 : 429–434

Johnsen SJ, Dansgaard W, White JWC (1989) The origin of Arctic precipitation under present and glacial conditions. Tellus (Ser B) 41 : 452–468

Johnsen SJ, Clausen HB, Dansgaard W, Fuhrer K, Gundestrup N, Hammer CU, Iversen P, Jouzel J, Stauffer B, Steffensen JP (1992) Irregular interstadials recorded in a new Greenland ice core. Nature 359 : 311–313

Jouzel J, Barkov NI, Barnola JM, Bender M, Chappellaz J, Genthon C, Kotlyakov M, Lipenkov V, Lorius C, Petit J-R, Raynaud D, Raisbeck G, Ritz C, Sowers T, Stievenard M, Yiou F, Yiou P (1993) Extending the Vostok ice-core record of paleoclimate to the penultimate glacial period. Nature 364 : 407–412

Jouzel J, Merlivat L, Lorius C (1982) Deuterium excess in an East Antarctic ice core suggests higher relative humidity at the oceanic surface during the last glacial maximum. Nature 299 : 688–691

Jouzel J, Lorius C, Petit J-R, Genthon C, Barkov NI, Kotlyakov VM, Petrov VM (1987) Vostok ice core: a continuous isotope temperature record over the last climatic cycle (160 000 years). Nature 329 : 403–408

Jouzel J, Petit J-R, Barkov NI, Barnola J-M, Chappelaz J, Ciais P, Kotlyakov VM, Lorius C, Petrov VN, Raynaud D, Ritz C (1992) The last deglaciation in Antarctica: further evidence of a "Younger Dryas" type climatic event. In: Bard E, Broecker WS (eds) The last deglaciation: absolute and radiocarbon chronologies. Vol I 2 of NATO ASI, Springer-Verlag, Berlin, Heidelberg, New York, pp. 229–266

Keigwin LD, Lehman SJ (1994) Deep circulation change linked to Heinrich event 1 and Younger Dryas in a middepth North Atlantic core. Paleoceanography 9 : 185–194

Keigwin LD, Jones GA, Lehman SJ (1991) Deglacial meltwater discharge, North Atlantic deep circulation and abrupt climate change. J Geophys Res 96 : 16 811–16 826

Kendall M, Gibbons JD (1990) Rank correlation methods - Fifth edn, Oxford University Press, New York

Kitagawa H, van der Plicht J (1998) Atmospheric radiocarbon calibration to 45 000 y BP: late glacial fluctuations and cosmogenic isotope production. Science 279 : 1187–1190

Kleypas JA (1997) Modeled estimates of global reef habitat and carbonate production since the last glacial maximum. Paleoceanography 12 : 533–545

Labracherie M, Labeyrie LD, Duprat J, Bard E, Arnold M, Pichon J-J, Duplessy J-C (1989) The last deglaciation in the Southern Ocean. Paleoceanography 4 : 629–638

Laj C, Mazaud A, Duplessy J-C (1996) Geomagnetic intensity and $^{14}C$ abundance in the atmosphere and ocean during the last 50 ky. Geophys Res Lett 23 : 2045–2048

Lehman SJ, Keigwin LD (1992) Sudden changes in North Atlantic circulation during the last deglaciation. Nature 356 : 757–762

Leuenberger M, Siegenthaler U, Langway CC (1992) Carbon isotope composition of atmospheric $CO_2$ from an Antarctic ice core. Nature 357 : 488–490

Lorius C, Jouzel J, Ritz C, Merlivat L, Barkov NI, Korotkevich YS, Kotlyakov VM (1985) A 150 000-year climatic record from Antarctic ice. Nature 316 : 591–596

Lorius C, Merlivat L, Jouzel J, Pourchet M (1979) A 30 000 y isotope climatic record from Antarctic ice. Nature 280 : 644–648

Mackensen A, Hubberten H-W, Bickert T, Fisher G, Fütterer DK (1993) The $\delta^{13}C$ in benthic foraminiferal tests of *Fontbotia wuellerstorfi* (Schwager) relative to the $\delta^{13}C$ of dissolved inorganic carbon in Southern Ocean deep water: implications for glacial ocean circulation models. Paleoceanography 8 : 587–610

Manabe S, Stouffer RJ (1993) Century-scale effects of increased atmospheric $CO_2$ on the ocean-atmosphere system. Nature 364 : 215–218

Manabe S, Stouffer RJ (1995) Simulation of abrupt climate change induced by freshwater input to the North Atlantic Ocean. Nature 378 : 165–167

Manabe S, Stouffer RJ (1997) Coupled ocean-atmosphere model response to freshwater input: comparison to Younger Dryas event. Paleoceanography 12 : 321–336

Mangerud J, Anderson ST, Berglund BE, Donner JJ (1974) Quaternary stratigraphy of norden, a proposal for terminology and classification. Boreas 3 : 109–127

Marchal O, Stocker TF, Joos F (1998a) A latitude-depth, circulation-biogeochemical ocean model for paleoclimate studies. Development and sensitivities. Tellus (Ser. B) 50 : 290–316

Marchal O, Stocker TF, Joos F (1998b) Impact of oceanic reorganizations on the ocean carbon cycle and atmospheric carbon dioxide content. Paleoceanography 13 : 225–244

Marchitto TM, Curry WB, Oppo DW (1998) Millennial-scale changes in North Atlantic circulation since the last glaciation. Nature 393 : 557–561

McCorkle D, Martin PA, Lea DW, Klinkhammer GP (1995) Evidence of a dissolution effect on benthic foraminiferal shell chemistry: $\delta^{13}C$, Cd/Ca Ba/Ca, and Sr/Ca results from the Ontong Java Plateau. Paleoceanography 10 : 699–714

Merlivat L, Jouzel J (1979) Global climatic interpretation of the deuterium-oxygen 18 relationship for precipitation. J Geophys Res 84 : 5029–5033

Mikolajewicz U (1996) A meltwater induced collapse of the 'conveyor belt' – thermohaline circulation and its influence on the distribution of $\Delta^{14}C$ and $\delta^{18}O$. Max-Planck-Inst. für Meteorologie Hamburg, Germany, Tech Rep 189 : 1–25

Mikolajewicz U, Crowley TJ, Schiller A, Voss R (1997) Modelling teleconnections between the North Atlantic and North Pacific during the Younger Dryas. Nature 387 : 384–387

Neftel A, Oeschger H, Staffelbach T, Stauffer B (1988) $CO_2$ record in the Byrd ice core 50 000-5000 y BP. Nature 331 : 609–611

Opdyke BN, Walker JCG (1992) Return to the coral reef hypothesis: basin to shelf partitioning of $CaCO_3$ and its effects on atmospheric $CO_2$. Geology 20 : 733–736

Peteet D (1995) Global Younger Dryas? Quat Int 28 : 93–104

Ruddiman WF, McIntyre A (1981) The North Atlantic Ocean during the last deglaciation. Paleogeogr Paleoclimatol Paleocol 35 : 145–214

Sarnthein M, Winn K, Jung SJA, Duplessy J-C, Labeyrie L, Erlenkeuser H, Ganssen G (1994) Changes in east Atlantic deepwater circulation over the last 30 000 years: eight time slice reconstructions. Paleoceanography 9 : 209–267

Schiller A, Mikolajewicz U, Voss R (1997) The stability of the North Atlantic thermohaline circulation in a coupled ocean-atmosphere general circulation model. Clim Dyn 13 : 325–347

Severinghaus JP, Sowers T, Brook EJ, Alley RB, Bender ML (1998) Timing of abrupt climate change at the end of the Younger Dryas interval from thermally fractionated gases in polar ice. Nature 391 : 141–146

Siegenthaler U, Oeschger H (1987) Biospheric $CO_2$ emissions during the past 200 years reconstructed by convolution of ice core data. Tellus (Ser B) 39 : 140–154

Steig EJ, Brook EJ, White JWC, Sucher CM, Bender ML, Lehman SJ, Morse DL, Waddington ED, Clow GD (1998) Synchronous climate changes in Antarctica and the North Atlantic. Science 282 : 92–95

Stocker TF, Schmittner A (1997) Influence of $CO_2$ emission rates on the stability of the thermohaline circulation. Nature 388 : 862–865

Stocker TF, Wright DG (1996) Rapid changes in ocean circulation and atmospheric radiocarbon. Paleoceanography 11 : 773–796.

Stocker TF, Wright DG, Mysak LA (1992) A zonally averaged, coupled ocean-atmosphere model for paleoclimate studies. J Clim 5 : 773–797.

Stuiver M, Braziunas TF (1989) Atmospheric $^{14}C$ and century-scale solar oscillations. Nature 338 : 405–408.

Stuiver M, Braziunas T, Becker B, Kromer B (1991) Climatic, solar, oceanic, and geomagnetic influences on late-glacial and Holocene atmospheric $^{14}C/^{12}C$ change. Quat Res 35 : 1–24.

Takahashi T, Olafsson J, Goddard G, Chipman DW, Sutherland SC (1993) Seasonal variation of $CO_2$ and nutrients in the

high-latitude surface oceans: a comparative study. Global Biogeochem Cycles 7:843–878

Tans PP, Fung IY, Takahashi T (1990) Observational constraints on the global atmospheric $CO_2$ budget. Science 247:1431–1438

Tric E, Valet J-P, Tucholka P, Paterne M, Labeyrie L, Guichard F, Tauxe L, Fontugne M (1992) Paleointensity of the geomagnetic field during the last 80 000 years. J Geophys Res 97:9337–9351

Veum T, Jansen E, Arnold M, Beyer I, Duplessy J-C (1992) Water mass exchange between the North Atlantic and the Norwegian Sea during the past 28 000 years. Nature 356:783–785

Wright DG, Stocker TF (1991) A zonally averaged ocean model for the thermohaline circulation, Part I: model development and flow dynamics. J Phys Oceanogr 21:1713–1724

Wright DG, Stocker TF (1992) Sensitivities of a zonally averaged global ocean circulation model. J Geophys Res 97:12 707–12 730

Wright DG, Stocker TF (1993) Younger Dryas experiments. In: Peltier WR (ed) Ice in the climate system NATO ASI Ser., Ser. I, 12, pp 395–416